Neuropharmacology 175 (2020) 108194

Contents lists available at ScienceDirect

Neuropharmacology

journal homepage: www.elsevier.com/locate/neuropharm

Coronaridine congeners decrease neuropathic pain in mice and inhibit α9α10 nicotinic acetylcholine receptors and $Ca_V2.2$ channels

Hugo R. Arias[a,**,1], Han-Shen Tae[b,*,1], Laura Micheli[c], Arsalan Yousuf[b], Carla Ghelardini[c], David J. Adams[b], Lorenzo Di Cesare Mannelli[c]

[a] Department of Pharmacology and Physiology, Oklahoma State University College of Osteopathic Medicine, Tahlequah, OK, USA
[b] Illawarra Health and Medical Research Institute (IHMRI), University of Wollongong, Wollongong, NSW, 2522, Australia
[c] Department of Neurosciences, Psychology, Drug Research and Child Health (NEUROFARBA), Section of Pharmacology and Toxicology, University of Florence, 50139, Florence, Italy

HIGHLIGHTS

- (±)-18-MC and (+)-catharanthine decrease drug-induced neuropathic pain.
- Both drugs inhibit α9α10 at higher potency than that for α3β4 and α4β2 nAChRs.
- Both drugs directly inhibit $Ca_V2.2$ channels but not *via* activation of $GABA_BR$.
- Their analgesic mechanisms may involve the inhibition of α9α10 nAChRs and/or $Ca_V2.2$ channels.

ARTICLE INFO

Keywords:
Coronaridine congeners
18-Methoxycoronaridine
(+)-catharanthine
Neuropathic pain
Nicotinic acetylcholine receptors
Voltage-gated ($Ca_V2.2$) calcium channels

ABSTRACT

The primary aim of this study was to determine the anti-neuropathic activity of (±)-18-methoxycoronaridine [(±)-18-MC] and (+)-catharanthine in mice by using the oxaliplatin-induced neuropathic pain paradigm and cold plate test. The results showed that both coronaridine congeners induce anti-neuropathic pain activity at a dose of 72 mg/kg (*per os*), whereas a lower dose (36 mg/kg) of (+)-catharanthine decreased the progress of oxaliplatin-induced neuropathic pain. To determine the underlying molecular mechanism, electrophysiological recordings were performed on α9α10, α3β4, and α4β2 nAChRs as well as voltage-gated calcium ($Ca_V2.2$) channels modulated by G protein-coupled γ-aminobutyric acid type B receptors ($GABA_BRs$). The results showed that (±)-18-MC and (+)-catharanthine competitively inhibit α9α10 nAChRs with potencies higher than that at α3β4 and α4β2 nAChRs and directly block $Ca_V2.2$ channels without activating $GABA_BRs$. Considering the potency of the coronaridine congeners at Cav2.2 channels and α9α10 nAChRs, and the calculated brain concentration of (+)-catharanthine, it is plausible that the observed anti-neuropathic pain effects are mediated by peripheral and central mechanisms involving the inhibition of α9α10 nAChRs and/or $Ca_V2.2$ channels.

1. Introduction

In general, coronaridine congeners (e.g., (±)-18-methoxycoronaridine [(±)-18-MC] alleviate drug craving and decrease relapse in humans and diminish drug self-administration in animals (Maisonneuve and Glick, 2003). Although preliminary results suggest that (±)-18-MC has antidepressant, anxiolytic and anti-obesity activities (Maisonneuve and Glick, 2003; Taraschenko et al., 2008), and (+)-cantharanthine has sedative activity (Arias et al., 2020), there is no study demonstrating its potential anti-pain (i.e., analgesic) activity. In this regard, the primary objective of this study was to determine the anti-neuropathic pain activity of (±)-18-MC and (+)-catharanthine in

Abbreviations: nAChR, nicotinic acetylcholine receptor; $GABA_BR$, γ-aminobutyric acid type B receptor; $Ca_V2.2$, voltage-gated N-type calcium channel; ACh, acetylcholine; (±)-18-MC, (±)-18-methoxycoronaridine; (+)-catharanthine, (+)-3,4-didehydrocoronaridine; EC_{50}, ligand concentration that produces half-maximal excitatory response; IC_{50}, ligand concentration that produces half-maximal inhibition; n_H, Hill coefficient

* Corresponding author.
** Corresponding author.
E-mail addresses: hugo.arias@okstate.edu (H.R. Arias), hstae@uow.edu.au (H.-S. Tae).
[1] Both authors contributed equally.

https://doi.org/10.1016/j.neuropharm.2020.108194
Received 31 January 2020; Received in revised form 4 June 2020; Accepted 8 June 2020
Available online 12 June 2020

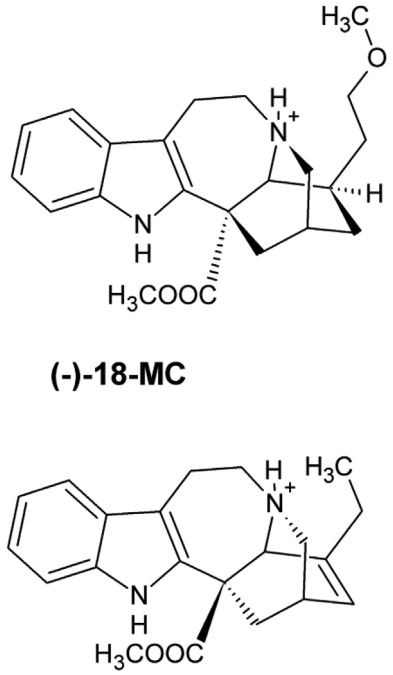

Fig. 1. Molecular structure of (−)-18-MC [(−)-18-methoxycoronaridine] and (+)-catharanthine [(+)-3,4-didehydrocoronaridine] in the protonated state (i.e., at physiological pH).

mice by using the oxaliplatin-induced neuropathic pain paradigm and cold plate test (Cavaletti et al., 2001).

Pharmacological studies performed to date indicate that (±)-18-MC and (+)-catharanthine (Fig. 1) behave as noncompetitive antagonists of several neuronal nicotinic acetylcholine receptor (nAChR) subtypes with the following human receptor selectivity sequence: α3β4 > α4β2 > α7 (Arias et al., 2017, 2010; 2015). The receptor selectivity toward α3β4-containing (α3β4*) nAChRs expressed in the habenula has been ascribed as responsible for the anti-addictive efficacy and safer toxicological profile observed for (±)-18-MC (Arias et al., 2017; Maisonneuve and Glick, 2003). Nevertheless, to date, there has been no study of the activity of coronaridine congeners at α9-containing (α9*) nAChRs. These receptors are expressed in outer hair cells of the cochlea (Elgoyhen et al., 2009), various immune cells (Fujii et al., 2017), and have been reported to be involved in pain related processes (Christensen et al., 2017; Hone and McIntosh, 2018; McIntosh et al., 2009; Romero et al., 2017). Thus, in this study the activity of (±)-18-MC and (+)-catharanthine was investigated on human (h) and rat (r) α9α10, α3β4, and α4β2 nAChRs by using the two-electrode voltage clamp recording technique. Given that $Ca_V2.2$ channels have been implicated in pain signaling (Lee, 2013; Winquist et al., 2005; Zamponi et al., 2015), the activity of both coronaridine congeners was also investigated on $hCa_V2.2$ channels alone or co-expressed with $hGABA_BRs$, by using whole-cell patch clamp recording technique.

Our findings showed that (±)-18-MC and (+)-catharanthine decrease drug-induced neuropathic pain in mice as well as inhibit α9α10 nAChRs and $Ca_V2.2$ channels at clinically relevant concentrations. This study provides an initial understanding of the neurochemical mechanisms underlying the anti-neuropathic pain activity of these compounds.

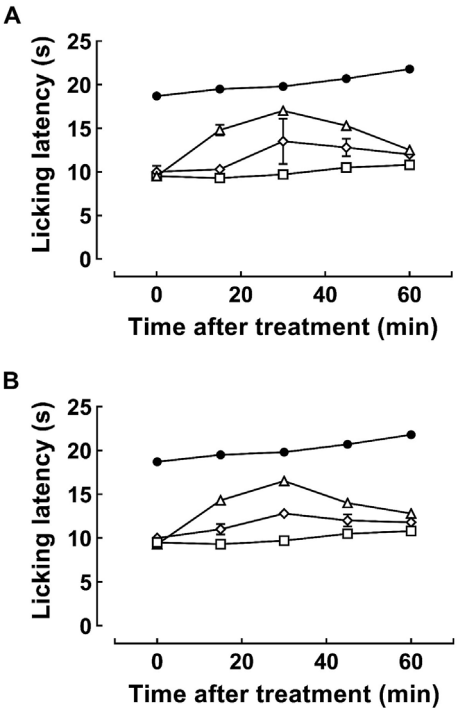

Fig. 2. Effect of (±)-18-MC (A) or (+)-catharanthine (B) on oxaliplatin-induced neuropathic pain in mice. Mice (n = 10/condition) were administered (i.p.) with 2.4 mg/kg oxaliplatin (□) during days 1–3, 6–10, and 13–14. On day 15, mice were administered (p.o.) with (±)-18-MC (A) or (+)-catharanthine (B) at doses of 36 (◊) and 72 (Δ) mg/kg, respectively, and the pain threshold subsequently determined by using the cold plate test. The time latency (mean ± SEM) for the first signs of pain-related behavior (i.e., lifting and licking of the hind paw) was recorded after 15, 30, 45, and 60 min after treatment. Bonferroni post-hoc analyses indicated that: oxaliplatin + vehicle treated animals (□) developed neuropathic pain during the whole testing time (i.e., 0–60 min) [$P < 0.05$ vs vehicle + vehicle treated animals (●)]; and that 72 (Δ), but not 36 (◊), mg/kg congener + oxaliplatin decreased neuropathic pain between 15 and 45 min [$P < 0.05$ vs oxaliplatin + vehicle treated animals (□)].

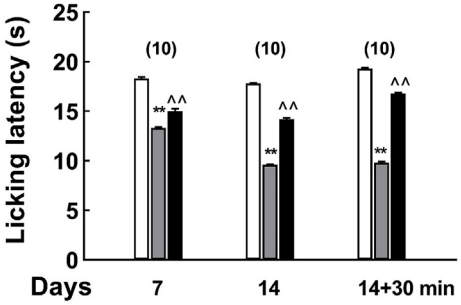

Fig. 3. (+)-Catharanthine reduced the development of oxaliplatin-induced neuropathic pain in mice. Mice (n = 10/condition) were administered (i.p.) with 2.4 mg/kg oxaliplatin (grey) or co-administered with 36 mg/kg (+)-catharanthine (p.o.) (black) using the same protocol described in Fig. 2. Pain threshold (mean ± SEM) was assessed by the cold plate test on day 7 and 14, respectively, 24 h after the last injection. Bonferroni post-hoc analyses indicated that oxaliplatin + vehicle induced neuropathic pain (i.e., decreased licking latency) after 7 and 14 days of treatment [Both $^{**}P < 0.05$ vs vehicle + vehicle treated mice (white)], whereas co-administration with (+)-catharanthine (black) decreased (i.e., increased licking latency) the progress of oxaliplatin-induced neuropathic pain (grey) after 7 and 14 days of co-treatment ($^{\wedge\wedge}P < 0.05$ for both). Thirty minutes after a new administration of 36 mg/kg (+)-catharanthine on day 14 (i.e., 14 + 30 min), a slightly higher increase in the licking latency was observed ($^{\wedge}P < 0.05$).

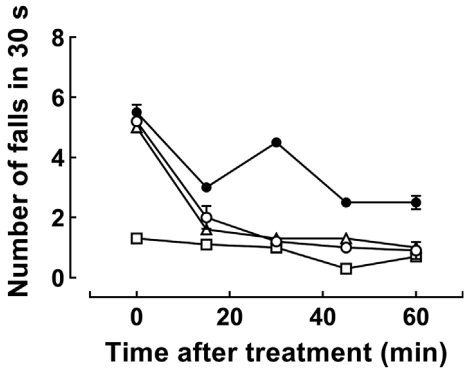

Fig. 4. Effect of (±)-18-MC, (+)-catharanthine (○) and oxaliplatin on mouse motor coordination determined by the rota-rod test. Mice (n = 10/condition) were treated (i.p.) with 2.4 mg/kg oxaliplatin or vehicle for 14. On day 15, animals were subsequently administered (p.o.) with 72 mg/kg of either (±)-18-MC (Δ), (+)-catharanthine (○) or vehicle and the roat-rod test was subsequently assessed. Bonferroni post-hoc analyses of the results (mean ± SEM) indicated that oxaliplatin + vehicle (●) induced motor coordination impairment (i.e., increased number of falls in 30 s) during the whole testing time (i.e., 0–60 min) [$P < 0.05$ vs vehicle + vehicle treated animals (□)], whereas both (±)-18-MC (Δ) and (+)-catharanthine (○) improved the motor coordination impairment in oxaliplatin + vehicle treated animals (●) ($P < 0.05$), especially 30 min after the beginning of the test.

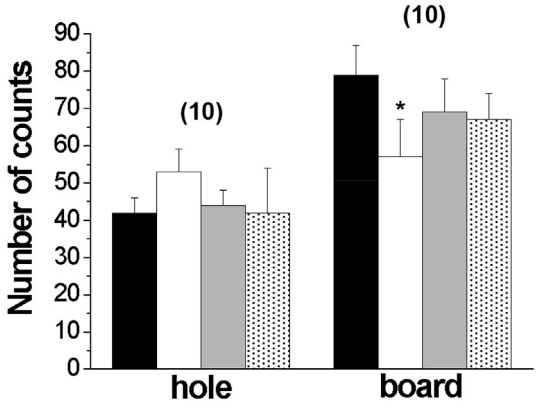

Fig. 5. Effect of (±)-18-MC, (+)-catharanthine and oxaliplatin on mouse spontaneous mobility and exploratory activity determined by the hole-board test. Mice (n = 10/condition) were treated (i.p.) with 2.4 mg/kg oxaliplatin or vehicle for 14 days. On day 15, animals were subsequently treated (p.o.) with 72 mg/kg of (±)-18-MC (grey), (+)-catharanthine (dots) or vehicle, and the hole-board test was performed 25 min after treatment. Bonferroni post-hoc analyses of the results (mean ± SEM) indicated that oxaliplatin + vehicle (white) decreased spontaneous motility (i.e., decreased number of crossings through the board's surface for a total time of 5 min) (*$P < 0.05$), but not exploratory activity (i.e., similar number of hole explorations for a total time of 5 min), compared to vehicle + vehicle-treated animals (black). The spontaneous mobility and exploratory activity observed in congener + oxaliplatin-treated animals was not statistically different to that in oxaliplatin + vehicle-treated mice.

2. Materials and methods

2.1. Chemicals

Fetal bovine serum (FBS), acetylcholine chloride (ACh), (±)-baclofen, and BAPTA-AM were obtained from Sigma-Aldrich (St. Louis, MO, USA), whereas glucose and carboxymethyl cellulose were obtained from Sigma-Aldrich SRL (Milan, Italy). Oxaliplatin, was obtained from Carbosynth (Berkshire, UK). Gentamicin was obtained from Gibco (Grand Island, NY, USA). DMEM, GlutaMAX, penicillin, and streptomycin were purchased from Invitrogen Life Technologies (Carlsbad, CA, USA). Fetal bovine serum (FBS) for cell culture was obtained from Bovogen (East Keilor, VIC, Australia). Collagenase Type II was purchased from Worthington Biochemical Corp. (Lakewood, NJ, USA). CGP 55845 hydrochloride was purchased from Tocris Bioscience (Bristol, UK). (±)-18-Methoxycoronaridine hydrochloride [(±)-18-MC] was purchased from Obiter Research, LLC (Champaign, IL, USA). (+)-Catharanthine (base) was obtained from Cayman Chemicals (Ann Arbor, MI, USA). (+)-Catharanthine hydrochloride was a gift from Dr. Kuehne (University of Vermont, VT, USA). Salts were of analytical grade.

2.2. Animals

Male CD-1 albino mice (Envigo, Varese, Italy) weighing approximately 22–25 g at the beginning of the experimental procedure, were used in all experiments. Animals were housed in CeSAL (Centro Stabulazione Animali da Laboratorio, University of Florence) and used at least 1 week after their arrival. Ten mice were housed per cage (size 26 × 41 cm); animals were fed a standard laboratory diet and tap water *ad libitum*, and kept at 23 ± 1 °C with a 12 h light/dark cycle, light at 7 a.m. All animal manipulations were carried out according to the Directive 2010/63/EU of the European parliament and of the European Union council on the protection of animals used for scientific purposes. The ethical policy of the University of Florence complies with the Guide for the Care and Use of Laboratory Animals of the National Institutes of Health (USA). Formal approval to conduct the experiments described was obtained from the Animal Subjects Review Board of the University of Florence. All efforts were made to minimize animal suffering and to reduce the number of animals used.

Experiments were carried out between 9:00 a.m. and 6:00 p.m. in testing rooms adjacent to the animal rooms and were conducted by authorized investigators. Mice were tested only once and sacrificed immediately. Animal manipulations were approved by Reginal Ethical Committee for Animal Experimentation and performed according to the European Communities Council Directive (86/609/EEC + 2010/63/UE). A randomization of animals between groups and treatments was carried out. The investigators responsible for data analysis were blind to which animals represent treatments and controls.

2.3. Treatment of (±)-18-methoxycoronaridine and (+)-catharanthine on oxaliplatin-induced neuropathic pain

Mice (n = 10/condition) were intermittently administered *via* intraperitoneal (i.p.) injection with 2.4 mg/kg oxaliplatin (dissolved in 5% glucose solution) on days 1–3, 6–10, and 13–14, to develop neuropathic pain (Cavaletti et al., 2001). Control animals received an equivalent volume of vehicle. On day 15, (+)-catharanthine (HCl salt or base) and (±)-18-MC (HCl salt) [suspended in 1% carboxymethyl cellulose (i.e., vehicle)] were acutely administered [*per os* (p.o.)] at doses of 40 and 80 mg/kg (i.e., corresponding to 36 and 72 mg/kg of the respective bases). The pain threshold was subsequently determined by the cold plate test before and 15, 30, 45, and 60 min after treatment.

2.4. Co-treatment of (+)-catharanthine and oxaliplatin

To determine whether (+)-catharanthine decreases the development of neuropathic pain induced by oxaliplatin (n = 10/condition), mice were co-administered with 2.4 mg/kg oxaliplatin and an inactive dose of (+)-catharanthine (36 mg/kg; p.o.) following the same protocol as that for oxaliplatin alone. Pain threshold values corresponding to 7 and 14 days of co-treatment were determined 24 h after the last administration by using the cold plate test. In addition, 30 min after the last treatment/cold plate test, the anti-neuropathic pain activity of a subsequent administration of 36 mg/kg (+)-catharanthine was assessed.

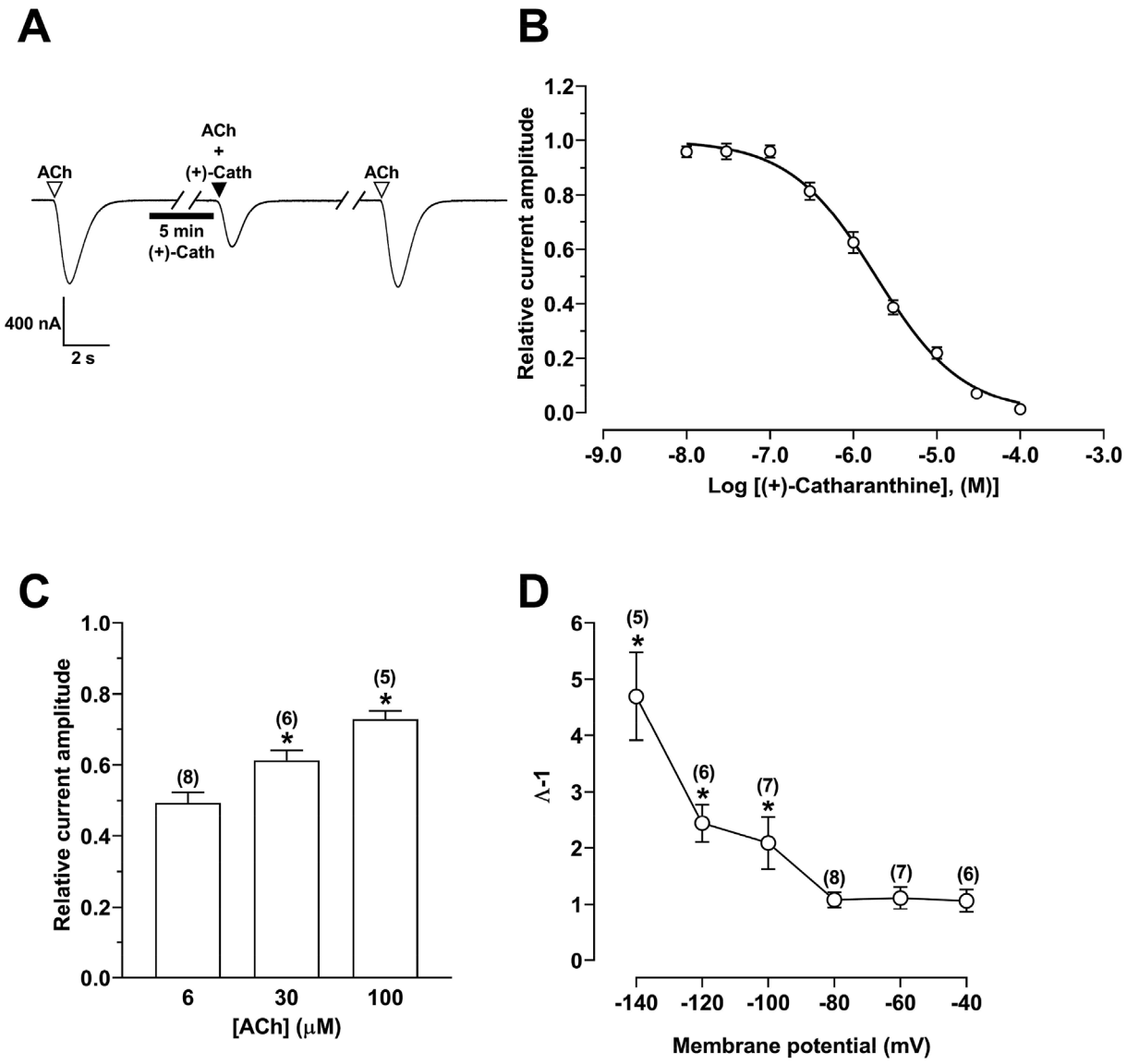

Fig. 6. Inhibitory activity of (+)-catharanthine at hα9α10 nAChRs. (A) Representative ACh (6 μM)-evoked hα9α10 nAChR currents obtained at −80 mV in the absence and presence of 1 μM (+)-catharanthine, and after drug washout. ▽, ACh alone; ▼, co-application of ACh + (+)-catharanthine after 5 min incubation (▬) with (+)-catharanthine alone; ▽, ACh alone after washout. (B) Concentration-response relationship for (+)-catharanthine-induced inhibition of ACh-evoked current amplitudes at hα9α10 nAChRs. Current amplitudes [mean ± SEM; n = 5–10] were normalized to the response elicited by 6 μM ACh alone (corresponding to its EC_{50} at hα9α10 nAChRs). The calculated IC_{50} and n_H values are summarized in Table 1 (C) (+)-Catharanthine (1.9 μM) inhibition of hα9α10 nAChRs obtained at three different ACh concentrations (i.e., 6, 30 and 100 μM) (mean ± SEM; n = 5–8). Unpaired Student's t-test analyses showed that the inhibition was significantly reduced at ACh concentrations ≥30 μM (*$P < 0.05$), suggesting a competitive mechanism. (D) (+)-Catharanthine (1.9 μM) inhibition of hα9α10 nAChRs as a function of membrane potential (mean ± SEM; n = 5–8). Unpaired Student's t-test analyses showed that the inhibition index (Λ−1) was greater at membrane potentials more negative than −80 mV (*$P < 0.05$).

2.5. Cold plate test

Each animal was placed in a stainless steel box (12 cm × 20 cm × 10 cm) with a cold plate as floor. The temperature of the cold plate was kept constant at 4 ± 1 °C. Pain-related behavior (licking of the hind paw) was observed and the time (s) of the first sign was recorded. The cut-off time of the latency of paw lifting or licking was set at 60 s (Di Cesare Mannelli et al., 2017).

2.6. Rota-rod test

The rota-rod test was used to determine the integrity of motor coordination in mice after drug treatment (Vaught et al., 1985). Mice (10/condition) were first treated (i.p.) with 2.4 mg/kg oxaliplatin or vehicle for 14 days as described previously. Rota-rod tests were performed on day 15, before and after each coronaridine congener or vehicle was acutely administered (p.o.) at the highest dose eliciting anti-neuropathic pain activity (72 mg/kg).

The apparatus used for the rota-rod tests consisted of a base platform and a rotating rod with a diameter of 3 cm and a non-slippery surface. The rod was placed at a height of 15 cm from the base. The rod, 30 cm in length, was divided into five equal sections by six disks. Thus, up to five mice were tested simultaneously on the apparatus, with a rod-rotating speed of 16 rpm (revolutions per minute). The integrity of motor coordination was assessed on the basis of the number of falls from the rod during the total time of the test (30 s). Mice scoring less than three and more than six falls in the pretest were rejected (20%) (Guerrini et al., 2017). The performance time was measured before

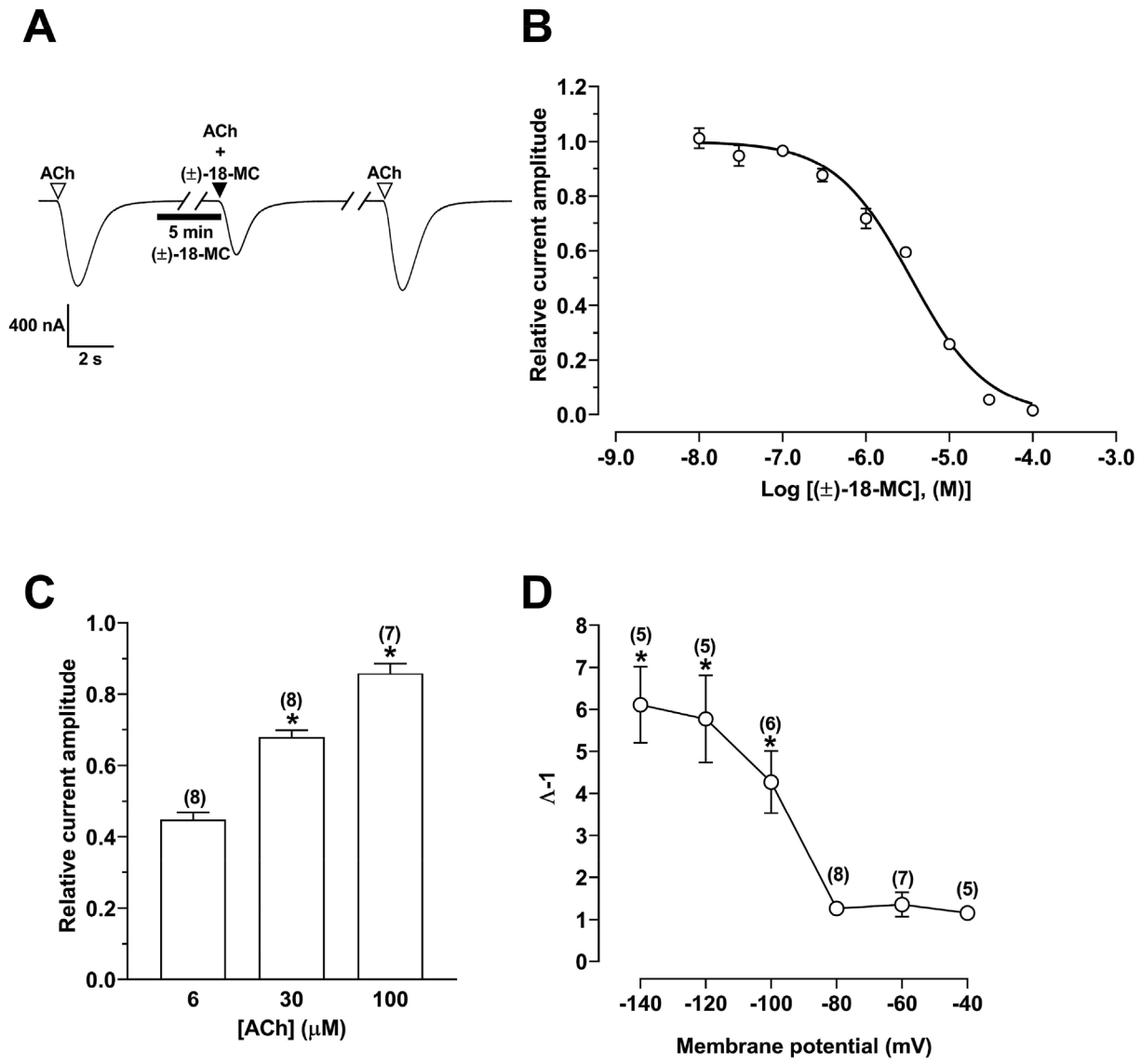

Fig. 7. Inhibitory activity of (±)-18-MC at hα9α10 nAChRs. (A) Representative ACh (6 μM)-evoked hα9α10 nAChR currents obtained at −80 mV in the absence and presence of 1 μM (±)-18-MC, and after drug washout. ▽, ACh alone; ▼, co-application of ACh + (±)-18-MC after 5 min incubation (▬) with (±)-18-MC alone; ▽, ACh alone after washout. (B) Concentration-response relationship for (±)-18-MC inhibition of ACh-evoked current amplitudes at hα9α10 nAChRs. Current amplitudes [mean ± SEM; n = 5–10] were normalized to the response elicited by 6 μM ACh alone (corresponding to its EC_{50} at hα9α10 nAChRs). The calculated IC_{50} and n_H values are summarized in Table 1 (C) (±)-18-MC (3.5 μM) inhibition of hα9α10 nAChRs obtained at three different ACh concentrations (i.e., 6, 30 and 100 μM) (mean ± SEM; n = 7–8). Unpaired Student's t-test analyses showed that the inhibition was significantly reduced at ACh concentrations ≥ 30 μM (*P < 0.05), suggesting a competitive mechanism. (D) (±)-18-MC (3.5 μM) inhibition of hα9α10 nAChRs as a function of membrane potential (mean ± SEM; n = 5–8). Unpaired Student's t-test analyses showed that the inhibition index (Λ - 1) was greater at membrane potentials more negative than −80 mV (*P < 0.05).

(pretest) and 15, 30, 45, and 60 min after the beginning of the test.

2.7. Hole-board test

The hole-board test was used to determine the spontaneous mobility (board) and the exploratory activity (hole) of mice after drug treatment (Guerrini et al., 2017). Mice (10/condition) were first treated (i.p.) with 2.4 mg/kg oxaliplatin for 14 days as described previously. On day 15, each coronaridine congener at the highest dose eliciting anti-neuropathic pain activity (72 mg/kg) or vehicle was acutely administered (p.o.) and after 25 min, the hole-board test was performed.

The apparatus consisted of a 40 cm square plane with 16 flush mounted cylindrical holes (3 cm diameter) distributed 4 × 4 in an equidistant, grid-like manner. Each mouse was placed on the center of the board and allowed to move about freely for a period of 5 min each. Two photobeams, crossing the plane from mid-point to mid-point of opposite sides, thus dividing the plane into 4 equal quadrants, automatically signaled the movement of the animal on the board surface for a total time of 5 min (i.e., spontaneous mobility). Miniature photoelectric cells, in each of the 16 holes, recorded hole exploration by the mice for a total time of 5 min. A higher or lower exploratory activity compared to control animals would suggest anxiolytic or anxiogenic activity, respectively, of the drugs (e.g., see Kumburovic et al., 2019).

2.8. Oocyte preparation and microinjection

Stage V-VI oocytes (Dumont's classification; 1200–1300 μm in diameter) were obtained from *Xenopus laevis*, defolliculated with 1.5 mg/mL collagenase Type II at room temperature (21–24 °C) for 1–2 h in OR-2 solution containing (in mM) 82.5 NaCl, 2 KCl, 1 $MgCl_2$, 5 HEPES, pH 7.4. Oocytes were injected with 35 ng of hα9α10 cRNA or 5 ng of either hα3β4, hα4β2, rα3β4 or rα9α10 cRNAs (concentration confirmed

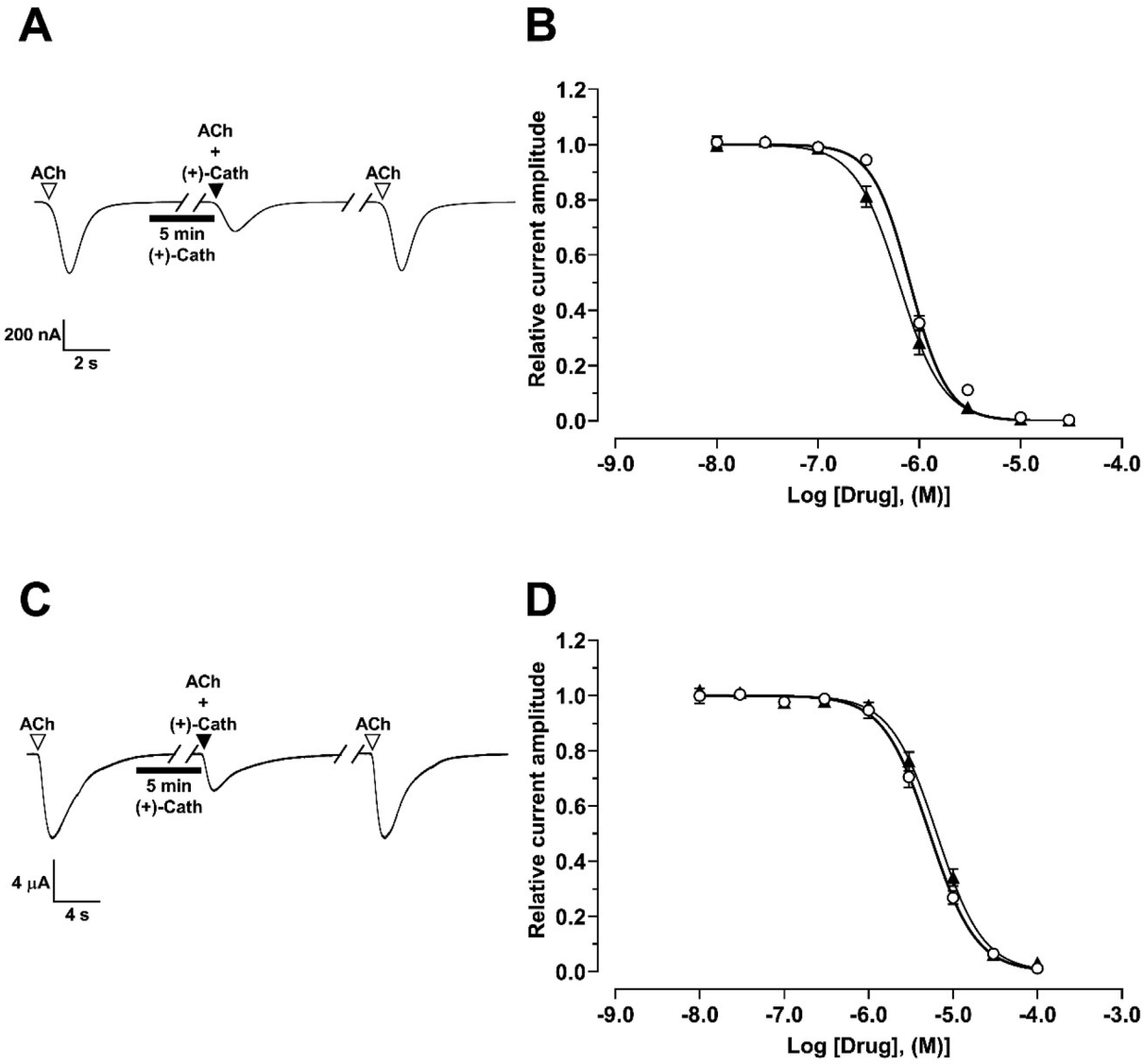

Fig. 8. Inhibitory activity of (+)-catharanthine and (±)-18-MC at (A,B) rα9α10 and (C,D) rα3β4 nAChRs. (A) Representative ACh (10 μM)-evoked rα9α10 nAChR currents mediated obtained at −80 mV in the absence and presence of 1 μM (+)-catharanthine. ▽ACh alone; ▼ co-application of ACh + (+)-catharanthine after 5 min incubation (▬) with (+)-catharanthine alone; ▽, ACh alone after washout. (B) Concentration-response relationships obtained for (+)-catharanthine (○) and (±)-18-MC (▲) inhibition of ACh-evoked current amplitudes at rα9α10 nAChRs. Current amplitudes [mean ± SEM; n = 5–6] were normalized to the response elicited by 10 μM ACh alone (corresponding to the EC_{50} value at rα9α10 nAChRs). (C) Representative ACh (100 μM)-evoked rα3β4 nAChR currents mediated by at −80 mV in the absence and presence of 10 μM (+)-catharanthine. ▽ ACh alone; ▼ co-application of ACh + (+)-catharanthine after 5 min incubation (▬) with (+)-catharanthine alone; ▽, ACh alone after washout. (D) Concentration-response relationships obtained for (+)-catharanthine (○) and (±)-18-MC (▲) inhibition of ACh-evoked current amplitudes at rα3β4 nAChRs. Current amplitudes (mean ± SEM; n = 5–7) were normalized to the response elicited by 100 μM ACh alone (corresponding to the EC_{50} value at rα3β4 nAChRs). The calculated IC_{50} and n_H values are summarized in Table 1.

spectrophotometrically and by gel electrophoresis) using glass pipettes (3-000-203 GX, Drummond Scientific Co., Broomall, PA, USA). For the synthesis of human nAChR subunit cRNAs, plasmid pT7TS constructs of hα3, hβ2, hβ4, hα9, and hα10 subunits were linearized with XbaI (NEB, Ipswich, MA, USA), and plasmid pSP64 construct of hα4 was linearized with BamHI (NEB) for *in vitro* T7 and SP6 mMessage mMachine®-cRNA transcription (AMBION, Foster City, CA, USA), respectively. For the synthesis of rat nAChR subunit cRNAs, plasmid pT7TS construct of rα3 and plasmid pNKS2 construct of rβ4 were linearized with XbaI for *in vitro* T7 and SP6 mMessage mMachine®-cRNA transcription, respectively. Plasmid pGEMHE and pSGEM constructs of rα9 and rα10, respectively, were linearized with NheI (NEB) for T7 mMessage mMachine®-cRNA transcription. The plasmid pT7TS hα3, hβ2, hα9, hα10 and rα3 constructs and plasmid pNKS2 rβ4 construct were generated in-house. The plasmid pSP64 construct of hα4 was sourced from Prof. A. Nicke (Ludwig Maximilian University of Munich), and plasmid pGEMHE rα9 and pSGEM rα10 constructs were kindly provided by Prof. M. Chebib (University of Sydney).

Oocytes were incubated at 18 °C in sterile ND96 solution composed of (in mM) 96 NaCl, 2 KCl, 1 $CaCl_2$, 1 $MgCl_2$, 5 HEPES, pH 7.4, supplemented with 5% FBS, 0.1 mg/mL gentamicin, and 100 U/mL penicillin-streptomycin. Female *X. laevis* were sourced from Nasco (Fort Atkinson, WI, USA) and a maximum of three frogs were kept in purpose-built 15 l aquarium at 20–26 °C with 12 h light/dark cycle at the University of Sydney Laboratory Animal Services facility. Oocytes were obtained from three frogs ~ five years old anaesthetized with 1.7 mg/mL ethyl 3-aminobenzoate methanesulfonate (pH 7.4 with $NaHCO_3$) and for recovery, post-surgery animals were placed in fresh water at level below the nostrils. Frogs were allowed to recover for a minimum of four months between surgeries. Terminal anaesthesia with 5 mg/mL

Table 1
Inhibitory potency of coronaridine congeners at several nAChRs and hCa$_V$2.2 channels.

Molecular Target	(+)-Catharanthine		(±)-18-MC	
	IC_{50} (μM)	n_H	IC_{50} (μM)	n_H
hα9α10 [a]	1.9 ± 0.1	0.83 ± 0.05	3.5 ± 0.2	0.95 ± 0.06
rα9α10 [b]	0.81 ± 0.03	2.36 ± 0.18	0.63 ± 0.03	2.00 ± 0.13
hα3β4 [c]	8.9 ± 0.7	0.99 ± 0.07	16.8 ± 1.2	1.09 ± 0.09
rα3β4 [d]	5.3 ± 0.2	1.58 ± 0.09	6.4 ± 0.3	1.59 ± 0.09
hα4β2 [e]	91.4 ± 17.4	0.66 ± 0.08	89.3 ± 7.1	1.15 ± 0.10
hCa$_V$2.2 [f]	1.3 ± 0.1	1.18 ± 0.09	3.0 ± 0.3	1.21 ± 0.14

n_H, Hill coefficient.
[a] Values obtained from Fig. 6B [(+)-Catharanthine] and Fig. 7B [(±)-18-MC] (n = 5–10), respectively.
[b] Values obtained from Fig. 9B (n = 5–6).
[c] Values obtained from Fig. 8B (n = 5–11).
[d] Values obtained from Fig. 9D (n = 5–7).
[e] Values obtained from Fig. 8D (n = 5–11).
[f] Values obtained from Fig. 10D (n = 4).

ethyl 3-aminobenzoate methanesulfonate (pH 7.4 with $NaHCO_3$) was performed on frogs at the sixth surgery. All procedures were approved by the University of Wollongong and University of Sydney Animal Ethics Committees.

2.9. Oocyte two-electrode voltage clamp recording

Electrophysiological recordings were carried out 2–7 days post cRNA microinjection. Two-electrode voltage clamp recordings of *X. laevis* oocytes expressing α9α10, α3β4, or α4β2 nAChRs were performed at room temperature using a GeneClamp 500B amplifier and pClamp 9 software interface (Molecular Devices, San Jose, CA, USA) at a holding potential −80 mV. In a series of experiments, the voltage-dependence of (+)-catharanthine and (±)-18-MC inhibition of hα9α10 nAChR was examined. Voltage-recording and current-injecting electrodes were pulled from GC150T-7.5 borosilicate glass (Harvard Apparatus, Holliston, MA, USA) and filled with 3 M KCl, giving resistances of 0.3–1 MΩ.

Oocytes expressing hα9α10 or rα9α10 nAChRs were incubated with 100 μM BAPTA-AM at 18 °C for ~3 h before recording and perfused with ND115 solution containing (in mM): 115 NaCl, 2.5 KCl, 1.8 $CaCl_2$, 10 HEPES, pH 7.4, whereas oocytes expressing either hα3β4, rα3β4 or hα4β2 nAChRs were perfused with ND96 solution, at a rate of 2 mL/min. Initially, oocytes were briefly washed with bath solution (ND115/ND96) followed by 3 applications of ACh at concentrations corresponding to the half-maximal effective concentration (i.e., EC_{50}) for hα9α10 (6 μM; Yu et al., 2018), hα3β4 (300 μM; Cuny et al., 2016), hα4β2 (3 μM; Liang et al., 2020), rα9α10 (10 μM; Halai et al., 2009) or rα3β4 (100 μM; Grishin et al., 2010) nAChRs, respectively, and 3 min washouts between ACh applications. Peak current amplitudes before and after incubation were measured using Clampfit 10.7 software (Molecular Devices) and the relative current amplitude, $I_{ACh+drug}/I_{ACh}$ (Λ), was used to assess drug's activity at nAChRs.

(+)-Catharanthine- and (±)-18-MC-induced inhibition of hα9α10 nAChRs was examined at different ACh concentrations (i.e., 6, 30 and 100 μM). Drug solutions were prepared in ND115/ND96 + 0.1% FBS. Oocytes were incubated with (+)-catharanthine or (±)-18-MC for 5 min with the perfusion system stopped, followed by co-application of ACh plus the coronaridine congener with flowing bath solution. Incubation with 0.1% FBS was performed to ensure that the FBS and the pressure of the perfusion system had no effect on the nAChRs. The voltage-dependence of ligand-induced hα9α10 nAChR inhibition was expressed as the inhibition index (Λ − 1), where values > 1 correspond to greater drug-induced inhibition.

2.10. Whole-cell patch clamp recording of HEK293T cells expressing Ca$_V$2.2 channels alone or co-expressed with GABA$_B$Rs

HEK293T cells (ATCC, Manassas, VA, USA) were cultured in DMEM supplemented with 10% FBS, 1% penicillin and streptomycin and 1x GlutaMAX at 37 °C in 5% CO_2. Cells were plated on 12 mm glass coverslips and transiently transfected using the calcium phosphate method. The tri-cistronic plasmid cDNA3.1 construct containing hGABA$_B$R1 and hGABA$_B$R2 subunits, and the green fluorescent protein (GFP), was co-transfected with plasmid cDNA3.1 constructs encoding hCa$_V$2.2 α1, α2δ1 and β3 subunits (all constructs were in-house generated) at 2 μg each. Plasmid construct of GFP (0.5 μg) was only co-transfected with pCDNA3.1 constructs of Ca$_V$2.2 α1, α2δ1 and β3 subunits for identification of transfected cells.

Whole-cell patch clamp recordings were performed within 24–48 h post-transfection at room temperature (21–23 °C). Cells were constantly superfused using a gravity flow perfusion system (AutoMate Scientific, Berkeley, CA, USA) with extracellular solution containing (in mM): 110 NaCl, 10 $BaCl_2$, 1 $MgCl_2$, 5 CsCl, 30 TEA-Cl, 10 glucose, 10 HEPES (pH 7.35 with TEA-OH; ~310 mOsmol/kg). Fire-polished borosilicate patch pipettes (2–3 MΩ) were filled with intracellular solution containing (in mM): 125 K-Gluconate, 5 NaCl, 2 $MgCl_2$, 5 EGTA, 10 HEPES (pH 7.2 with KOH; ~290 mOsmol/kg). Barium currents were elicited by a test depolarization to −10 mV (50 ms duration) from a holding potential of −80 mV at 0.1 Hz. Drug solutions were prepared in the external solution.

2.11. Statistical analysis of data

The concentration-response relationship for coronaridine congeners was analyzed by using the Prism 7 software (GraphPad, La Jolla, CA, USA) according to the Hill equation. The one-way ANOVA analyses and the subsequent Bonferroni post-hoc comparison of the behavioral data were performed by using the Origin 9 software (OriginLab Corp., Northampton, MA, USA). The electrophysiological results were analyzed by unpaired Student's t-tests. Values of $P \leq 0.05$ were considered statistically significant.

3. Results

3.1. Coronaridine congeners decrease oxaliplatin-induced neuropathic pain

A single administration of either (±)-18-MC or (+)-catharanthine (Fig. 2A and B) reduced neuropathic pain (i.e., cold hypersensitivity) induced by intermittent treatment with 2.4 mg/kg oxaliplatin. On day 15, when neuropathy was well established, each compound was acutely administered at doses of 36 and 72 mg/kg, and its respective activity determined by using the cold plate test. Bonferroni post-hoc analyses indicated that both drugs significantly decreased neuropathic pain only at 72 mg/kg (Fig. 2A and B). The kinetics results indicated that this effect is elicited between 15 and 45 min after administration, with a peak at 30 min.

3.2. Cantharanthine decreased the development of oxaliplatin-induced neuropathic pain in mice

To determine whether (+)-catharanthine decreases the development of oxaliplatin-induced neuropathic pain, mice were co-administered with an inactive dose of this ligand (36 mg/kg) and 2.4 mg/kg oxaliplatin using the same protocol as described for oxaliplatin alone (Fig. 3A). Bonferroni post-hoc analyses indicated that the oxaliplatin-induced neuropathic pain observed after 7 and 14 days of treatment ($P < 0.05$; compared to vehicle-treated animals) was significantly decreased when oxaliplatin was co-administered with (+)-catharanthine for 7 and 14 days, respectively ($P < 0.05$ for both) (Fig. 3). In addition, a slightly higher decrease in neuropathic pain was observed

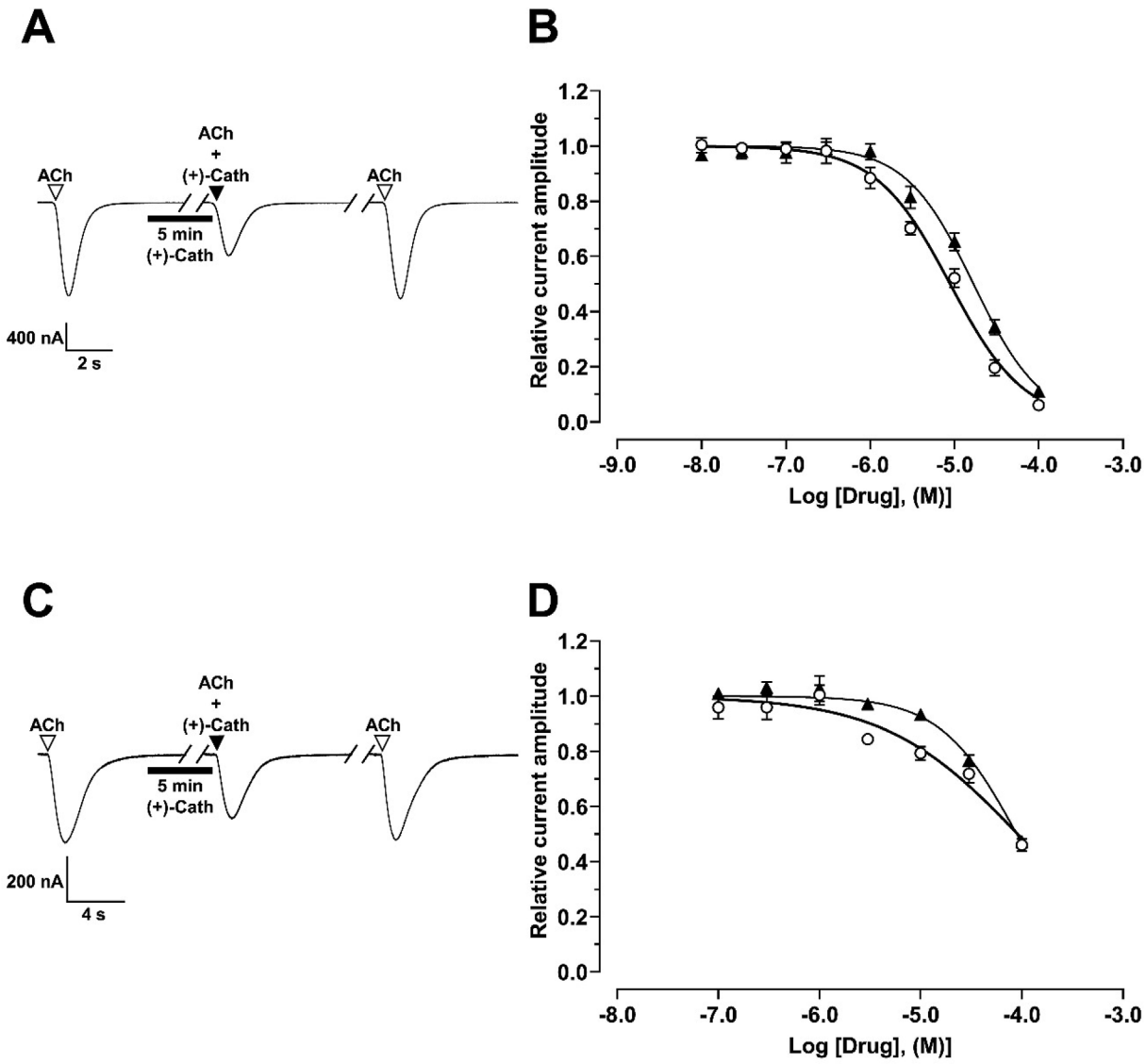

Fig. 9. Inhibitory activity of (+)-catharanthine and (±)-18-MC at hα3β4 and hα4β2 nAChRs. (A) Representative ACh (300 μM)-evoked hα3β4 nAChR currents obtained at −80 mV in the absence and presence of 10 μM (+)-catharanthine. ▽ ACh alone; ▼ co-application of ACh + (+)-catharanthine after 5 min incubation (▬) with (+)-catharanthine alone; ▽, ACh alone after washout. (B) Concentration-response relationships obtained for (+)-catharanthine- (○) and (±)-18-MC-induced (▲) inhibition of ACh-evoked current amplitudes at hα3β4 nAChRs. Current amplitudes [mean ± SEM; n = 5–11] were normalized to the response elicited by 300 μM ACh alone (corresponding to the EC_{50} value at hα3β4 nAChRs). (C) Representative ACh (3 μM)-evoked hα4β2 nAChR currents at −80 mV in the absence and presence of 10 μM (+)-catharanthine. ▽ ACh alone; ▼ co-application of ACh + (+)-catharanthine after 5 min incubation (▬) with (+)-catharanthine alone; ▽, ACh alone after washout. (D) Concentration-response relationships obtained for (+)-catharanthine- (○) and (±)-18-MC-induced (▲) inhibition of ACh-evoked current amplitude at hα4β2 nAChRs. Current amplitudes [mean ± SEM; n = 5–11] were normalized to the response elicited by elicited by 3 μM ACh alone (corresponding to the EC_{50} value at hα4β2 nAChRs). The calculated IC_{50} and n_H values are summarized in Table 1.

30 min after a new administration of (+)-catharanthine on day 14 (i.e., 14 + 30 min) (Fig. 3).

3.3. Effect of coronaridine congeners on mouse motor coordination

To determine the integrity of motor coordination in mice treated with oxaliplatin (alone) or subsequently administered with either (±)-18-MC or (+)-catharanthine (72 mg/kg), the endurance time of each mouse in the rota-rod (i.e., number of falls within 30 s) was evaluated before and 15, 30, 45, and 60 min after drug treatment (Fig. 4). Bonferroni post-hoc analyses demonstrated that oxaliplatin (alone) induced motor coordination impairment during the whole testing time (i.e., 0–60 min) compared to vehicle + vehicle-treated animals ($P < 0.05$) (Fig. 4). Interestingly, both (±)-18-MC and (+)-catharanthine improved the motor coordination impairment induced by oxaliplatin, especially 30 min after the beginning of the test ($P < 0.05$) (Fig. 4). The number of falls in oxaliplatin/congener-treated mice were similar to that observed in vehicle + vehicle-treated animals, suggesting that coronaridine congeners do not induce *per se* any further motor coordination impairment. Since (+)-catharanthine (63 mg/kg) decreased mouse locomotor activity due to its sedative effect (Arias et al., 2020), additional tests to determine the effect of coronaridine congeners (alone) on motor coordination cannot be accomplished.

3.4. Effect of coronaridine congeners and oxaliplatin on mouse spontaneous mobility and exploratory activity

To determine the spontaneous mobility and exploratory activity of mice treated with oxaliplatin (alone) or subsequently administered with

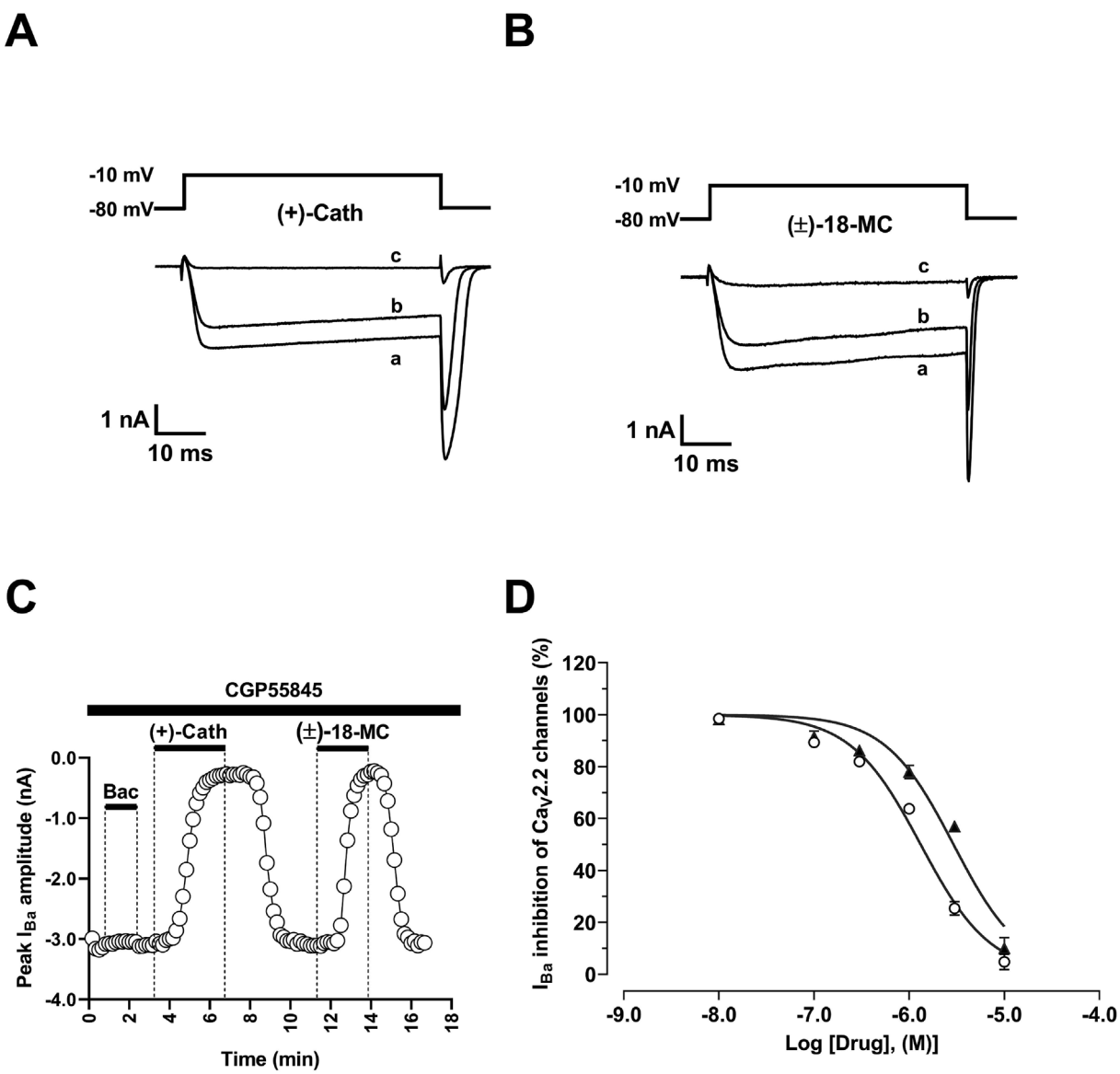

Fig. 10. Inhibitory activity of (+)-catharanthine and (±)-18-MC at $hCa_V2.2$ channels heterologously expressed alone or co-expressed with $hGABA_BRs$ in HEK293T cells. (A,B) Representative depolarization-activated Ba^{2+} currents (I_{Ba}) elicited from a holding potential of −80 mV to a test potential of −10 mV (50 ms duration; 0.1 Hz) from HEK293T cells co-expressing $Ca_V2.2$ channels and $GABA_BRs$ in the absence (a) and presence of 1 μM (b) and 10 μM (c) of (+)-catharanthine (A) and (±)-18-MC (B), respectively. (C) Time-dependent plot of Ba^{2+} current amplitudes before, during and upon washout of 50 μM baclofen (Bac), 10 μM (+)-catharanthine, and 10 μM (±)-18-MC in the continuous presence of 1 μM CGP55845. (D) Concentration-response relationships obtained for (+)-catharanthine- (○) and (±)-18-MC-induced (▲) inhibition of $hCa_V2.2$ channels expressed alone (mean ± SEM; n = 4). The calculated IC_{50} and n_H values are summarized in Table 1.

either (±)-18-MC or (+)-catharanthine (72 mg/kg) the hole-board test was assessed 25 min after treatment. Bonferroni post-hoc analyses indicated that oxaliplatin decreased spontaneous mobility (i.e., decreased the number of crossings through the board's surface for a total time of 5 min) ($P < 0.05$), but not exploratory activity (i.e., similar number of hole explorations for a total time of 5 min), compared to vehicle + vehicle-treated animals (Fig. 5). Coronaridine congeners neither improved the decreased spontaneous mobility nor affected the exploratory activity observed in oxaliplatin-treated animals (Fig. 5). The number of counts in oxaliplatin + congener-treated mice were similar to that observed in vehicle + vehicle-treated animals, suggesting that coronaridine congeners do not produce *per se* any further effect on mouse spontaneous mobility. Since (+)-catharanthine (63 mg/kg) decreased mouse locomotor activity due to its sedative effect (Arias et al., 2020), additional tests to determine the effect of coronaridine congeners on spontaneous mobility and exploratory activity cannot be accomplished.

3.5. Inhibitory activity of coronaridine congeners at human and rat nAChRs

The activity of both (+)-catharanthine and (±)-18-MC was tested at human and rat α9α10, α3β4, and human α4β2 nAChRs heterologously expressed in *X. laevis* oocytes using the two-electrode voltage clamp recording technique. At 1 μM, (+)-catharanthine (Fig. 6A) and (±)-18-MC (Fig. 7A) inhibited hα9α10 ACh-evoked currents by 37.5 ± 3.8% and 28.3 ± 3.7% (n = 6–7), respectively, in a reversible manner (upon washout). Similar results were obtained at rα9α10 nAChRs (Fig. 8A) which has ≥90% amino acid sequence homology to human α9 and α10 subunits. The concentration-response relationships showed that both (+)-catharanthine and (±)-18-MC (Fig. 8B) inhibit rα9α10 nAChRs with 2- to 5-fold higher potency than that at hα9α10 nAChRs (Figs. 6B and 7B), whereas (+)-catharanthine is ~2-fold more potent than (±)-18-MC at inhibiting hα9α10 nAChRs but equipotent at inhibiting rα9α10 nAChRs (Table 1). The calculated n_H values (Table 1) support a non-cooperative mechanism of action for both

compounds at hα9α10 nAChRs (i.e., n_H ~1), but a cooperative mechanism of action at rα9α10 nAChRs (i.e., n_H ~2).

To further investigate the inhibitory mechanism of coronaridine congeners at hα9α10 nAChRs, two approaches were used. First, the inhibitory activity of 1.9 μM (+)-catharanthine (Figs. 6C) and 1.0 μM (±)-18-MC (Fig. 7C) was determined at different ACh concentrations (i.e., 6, 30 and 100 μM). Student's t-test analyses indicated that the inhibition elicited by each drug was significantly reduced at ACh concentrations ≥30 μM. These results suggest a competitive mode of inhibition, although a non-competitive antagonism may likely be observed at higher concentrations. Second, the inhibition of hα9α10 nAChRs by (+)-catharanthine (Fig. 6D) and (±)-18-MC (Fig. 7D) at concentrations corresponding to their IC_{50} values (see Table 1) was determined at different membrane potentials. The inhibition of the ACh-evoked current amplitude by (+)-catharanthine and (±)-18-MC as a function of membrane potential indicated no significant voltage-dependence at membrane potentials less negative than −80 mV. Nevertheless, the inhibition (i.e., Λ−1) significantly increased at membrane potentials more negative than −80 mV, which may be a consequence of partially driving the drugs into the membrane electric field.

Given that both (+)-catharanthine and (±)-18-MC have been reported previously to inhibit hα3β4 and hα4β2 subtypes using fluorescence intracellular Ca^{2+} assays (Arias et al., 2017), they were also tested at hα3β4, rα3β4 and hα4β2 nAChRs expressed in *Xenopus* oocytes using the two-electrode voltage clamp recording technique. At 10 μM, (+)-catharanthine and (±)-18-MC reversibly inhibited ACh-evoked currents mediated by hα3β4 (Fig. 9A), rα3β4 nAChRs (Fig. 8C) and hα4β2 (Fig. 9C), respectively. The concentration-response relationships showed that coronaridine congeners inhibit rα3β4 (Fig. 8D) with greater potency than that for hα3β4 (Fig. 9B) and hα4β2 (Fig. 9D), that (+)-catharanthine is two-fold more potent than (±)-18-MC at both rα3β4 (Fig. 8D) and hα3β4 nAChRs (Fig. 9B), and that (+)-catharanthine selectivity for nAChR subtypes follows the sequence: hα9α10 > hα3β4 (4.7-fold) > hα4β2 (48-fold) (Table 1). The calculated near unity n_H values at hα3β4 and hα4β2 nAChRs (Table 1) support a non-cooperative mechanism of action for both compounds, whereas this mechanism is less clear at rα3β4 nAChRs (i.e., n_H ~1.5).

3.6. Activity of coronaridine congeners at $Ca_V2.2$ channels alone or coupled with $GABA_BRs$

Given that a class of analgesic α-conotoxins (e.g., Vc1.1, RgIA, and PeIA) have been shown to inhibit both α9α10 nAChRs and $Ca_V2.2$ channels *via* G protein-coupled $GABA_BR$ activation (Adams et al., 2012; Sadeghi et al., 2018), the effect of (+)-catharanthine and (±)-18-MC was investigated on $Ca_V2.2$ channels alone or co-expressed with $GABA_BRs$.

Depolarization-activated Ba^{2+} currents recorded from HEK293T cells transiently transfected with both $hCa_V2.2$ channels and $hGABA_BRs$ were reversibly inhibited by both (+)-catharanthine (Fig. 10A) and (±)-18-MC (Fig. 10B). However, the observed inhibition was not antagonized by the selective $GABA_BR$ antagonist, CGP55845 (1 μM) (Fig. 10C), unlike that observed for the $GABA_BR$ agonist, (±)-baclofen (Sadeghi et al., 2018). On the other hand, in HEK293T cells expressing $Ca_V2.2$ alone, both (+)-catharanthine and (±)-18-MC inhibited whole-cell Ba^{2+} currents in a concentration-dependent manner (Fig. 10D) with IC_{50}'s of 1.3 ± 0.1 μM (n = 4) and 3.0 ± 0.3 μM (n = 4), respectively (Table 1). These results demonstrate that coronaridine congeners inhibit $Ca_V2.2$ channels directly without involving modulation of the G protein-coupled $GABA_BR$.

4. Discussion

A primary objective of this study was to determine the anti-neuropathic pain (analgesic) activity mediated by two coronaridine congeners, (+)-catharanthine and (±)-18-MC, by using the oxaliplatin-induced neuropathic pain animal paradigm. To explore potential mechanisms of action, the inhibitory activity of these drugs was determined at human and rat nAChR subtypes as well as at $Ca_V2.2$ channels alone or co-expressed with $GABA_BRs$ using electrophysiological recording techniques. The voltage-dependence of inhibition by these drugs was also assessed at hα9α10 nAChRs.

Animal results showed that oxaliplatin treatment induced neuropathic pain and concomitantly decreased both motor coordination and spontaneous mobility, in agreement with previous studies (Christensen et al., 2017; Di Cesare Mannelli et al., 2017; Romero et al., 2017; Ta et al., 2009). Interestingly, both (±)-18-MC and (+)-catharanthine (72 mg/kg) were able to recover oxaliplatin-treated animals with neuropathic pain and motor impairment. Moreover, an inactive dose of (+)-catharanthine (36 mg/kg) was able to reduce the development of neuropathic pain after 7 or 14 days of co-treatment with oxaliplatin. This could be of clinical relevance in the prevention of chronic pain development. To our knowledge, this is the first report showing the anti-neuropathic pain activity of coronaridine congeners in mice. Our results also suggested that coronaridine congeners do not further increase the observed coordination and mobility impairments elicited by oxaliplatin, in agreement with previous studies in rats showing that (±)-18-MC (40 mg/kg) affected neither motor coordination nor locomotor activity (Maisonneuve and Glick, 2003 and references therein). On the other hand, neither oxaliplatin alone nor in combination with each congener affected mouse exploratory activity, suggesting that none of these treatments induced anxiolytic/anxiogenic activity. These results contrast with previous studies in rodents indicating that oxaliplatin induced anxiogenic activity (Kumburovic et al., 2019), whereas (±)-18-MC (40 mg/kg) induced anxiolytic activity (Maisonneuve and Glick, 2003).

Our electrophysiological results showed that (+)-catharanthine and (±)-18-MC competitively inhibit hα9α10 and rα9α10 nAChRs with higher potencies than that observed at hα3β4, rα3β4, and hα4β2 nAChRs. Since (±)-18-MC and (+)-catharanthine are 25- to 48-fold more potent at hα9α10 compared to that at hα4β2, we can rule out the possibility that the latter subtype is involved in the anti-neuropathic pain activity elicited by coronaridine congeners. Although a ≥ five-fold potency difference between α9α10 and α3β4 nAChRs could be clinically relevant, the brain concentration of (+)-catharanthine would need to be determined to assess the importance of each nAChR subtype in the observed anti-neuropathic pain activity elicited by coronaridine congeners.

Previous pharmacokinetics studies in rats showed a plasma concentration (i.e., [plasma]) of ~0.2 μM (+)-catharanthine after the p.o. administration of 15 mg/kg (Lin et al., 2015). Using the calculated blood-brain-barrier permeability value for (+)-catharanthine [LogBBB = Log ([brain]/[plasma]) = 0.338], a brain concentration of 0.43 μM was attained. Assuming that the plasma concentration will increase at higher doses, a plasma concentration of ~2 μM can be expected at the active dose used in our experiments, which is sufficient to inhibit mainly α9α10 nAChRs but also partially α3β4 nAChRs. Since α3β4* nAChRs are mainly expressed in the habenulo-interpeduncular pathway (Arias et al., 2017; Maisonneuve and Glick, 2003), whereas α9α10 nAChRs are mainly expressed in the cochlea (Elghoyen et al., 2009) and various immune cells (Zoli et al., 2018), it is possible that different but concomitant mechanisms, elicited by each nAChR subtype might be involved in the observed anti-neuropathic pain activity elicited by coronaridine congeners.

Previous studies supported the view that α9α10 nAChRs are involved in pain-related processes, and that selective ligands can be used for the treatment of neuropathic and inflammatory pain (Christensen et al., 2017; Hone and McIntosh, 2018; McIntosh et al., 2009; Romero et al., 2017). Since α9α10 nAChRs are expressed in peripheral immunocompetent cells (Zoli et al., 2018), the involvement of these nAChRs likely requires immune cell infiltration associated with the

painful nerve damage (Di Cesare Mannelli et al., 2014). Alternatively, the interaction between immune and nerve cells is gaining recognition in the pathophysiology of neuropathic pain (Lees et al., 2017). Thus, it is tempting to speculate that coronaridine congeners may modulate immune cell subsets that are likely to decrease the painful process.

Our study also demonstrates that both (±)-18-MC and (+)-catharanthine directly inhibit $hCa_V2.2$ channels without involving activation of the coupled $GABA_BR$. Interestingly, this mechanisms is different to that proposed for a class of analgesic α-conotoxins that also target α9α10 nAChRs (Adams et al., 2012; Sadeghi et al., 2018). Several coronaridine congeners, including (±)-18-MC, (+)-catharanthine, and (−)-ibogaine have been shown to inhibit a variety of voltage-gated ion channels, including L-type calcium channels, $hNa_V1.5$ sodium channels, and hERG potassium channels (Jadhav et al., 2013; Koenig et al., 2013). In particular, (−)-ibogaine had a comparatively higher inhibitory potency (IC_{50} = 53 μM) for calcium channels in guinea pig cardiomyocytes than that for $hCa_V1.2$ channels expressed in TSA-201 cells (163 μM) (Koenig et al., 2013). Nevertheless, to our knowledge, coronaridine congeners have not been tested on $Ca_V2.2$ channels. In our study, the IC_{50}'s determined at $hCa_V2.2$ channels for (±)-18-MC (3 μM) and (+)-catharanthine (1.3 μM) were similar to that observed for hα9α10 nAChRs, but significantly lower (10- to 100-fold) than that reported for voltage-gated sodium and calcium channels expressed in cardiomyocytes and vascular smooth muscle cells. Given that $Ca_V2.2$ is a recognized target for the treatment of chronic pain (Lee, 2013; Winquist et al., 2005; Zamponi et al., 2015), the mechanism of action of the coronaridine congeners may involve α9α10 nAChRs and/or Cav2.2 channels.

Our findings clearly show that (±)-18-MC and (+)-catharanthine decreased neuropathic pain in mice and inhibited not only hα9α10 nAChRs (at higher potency compared to other nAChR subtypes) but also $hCa_V2.2$ channels at clinically relevant concentrations. Both α9α10 nAChRs and $Ca_V2.2$ channels, and partially α3β4* nAChRs, might contribute through peripheral and central mechanisms to the observed anti-neuropathic activity mediated by coronaridine congeners.

Author contributions

HRA developed the concept. HRA, HT, LM, AY, CG and LDCM performed data analysis. LM performed the animal studies. CG supervised the animal studies. DJA supervised the electrophysiological experiments. HRA wrote the manuscript. HT, AY and LDCM wrote the methods and results of the electrophysiological and animal studies, respectively. LDCM assisted in developing the discussion. HRA, HT, CG, DJA and LDCM contributed to critical comments on the manuscript.

Declaration of competing interest

The authors declare that they have no conflict of interest.

Acknowledgements

This work was supported by grants from the Italian Ministry of Instruction, University and Research (MIUR) and the University of Florence (to C.G.), Australian Research Council (Discovery Project Grant DP150103990 to D.J.A.), and Oklahoma State University Center for Health Sciences (to H.R.A.). The authors thank to Dr. Kuehne (University of Vermont, VT, USA) for the (+)-catharanthine hydrochloride, Prof. A. Nicke (Ludwig Maximilian University of Munich) and Prof. M. Chebib (University of Sydney) for the plasmids, and Dr. M. Ortells (University of Moron, Argentina) for the calculation of the logBBB value for (+)-catharanthine.

References

Adams, D.J., Callaghan, B., Berecki, G., 2012. Analgesic conotoxins: block and G protein-coupled receptor modulation of N-type ($Ca_V2.2$) calcium channels. Br. J. Pharmacol. 166, 486–500. https://doi.org/10.1111/j.1476-5381.2011.01781.x.

Arias, H.R., Do Rego, J.L., Do Rego, J.C., Chen, Z., Anouar, Y., Scholze, P., Gonzales, E.B., Huang, R., Chagraoui, A., 2020. Coronaridine congeners potentiate $GABA_A$ receptors and induce sedative activity in mice in a benzodiazepine-insensitive manner. Prog. Neuro-Psychopharmacol. Biol. Psychiatry 101. https://doi.org/10.1016/j.pnpbp.2020.109930.

Arias, H.R., Jin, X., Feuerbach, D., Drenan, R.M., 2017. Selectivity of coronaridine congeners at nicotinic acetylcholine receptors and inhibitory activity on mouse medial habenula. Int. J. Biochem. Cell Biol. 92, 202–209. https://doi.org/10.1016/j.biocel.2017.10.006.

Arias, H.R., Rosenberg, A., Targowska-Duda, K.M., Feuerbach, D., Yuan, X.J., Jozwiak, K., Moaddel, R., Wainer, I.W., 2010. Interaction of ibogaine with human α3β4-nicotinic acetylcholine receptors in different conformational states. Int. J. Biochem. Cell Biol. 42, 1525–1535. https://doi.org/10.1016/j.biocel.2010.05.011.

Arias, H.R., Targowska-Duda, K.M., Feuerbach, D., Jozwiak, K., 2015. Coronaridine congeners inhibit human α3β4 nicotinic acetylcholine receptors by interacting with luminal and non-luminal sites. Int. J. Biochem. Cell Biol. 65, 81–90. https://doi.org/10.1016/j.biocel.2015.05.015.

Cavaletti, G., Tredici, G., Petruccioli, M.G., Donde, E., Tredici, P., Marmiroli, P., Minoia, C., Ronchi, A., Bayssas, M., Etienne, G.G., 2001. Effects of different schedules of oxaliplatin treatment on the peripheral nervous system of the rat. Eur. J. Canc. 37, 2457–2463. https://doi.org/10.1016/s0959-8049(01)00300-8.

Christensen, S.B., Hone, A.J., Roux, I., Kniazeff, J., Pin, J.P., Upert, G., Servent, D., Glowatzki, E., McIntosh, J.M., 2017. RgIA4 potently blocks mouse α9α10 nAChRs and provides long lasting protection against oxaliplatin-induced cold allodynia. Front. Cell. Neurosci. 11, 219. https://doi.org/10.3389/fncel.2017.00219.

Cuny, H., Kompella, S.N., Tae, H.S., Yu, R., Adams, D.J., 2016. Key structural determinants in the agonist binding loops of human β2 and β4 nicotinic acetylcholine receptor subunits contribute to α3β4 subtype selectivity of α-conotoxins. J. Biol. Chem. 291, 23779–23792. https://doi.org/10.1074/jbc.M116.730804.

Di Cesare Mannelli, L., Cinci, L., Micheli, L., Zanardelli, M., Pacini, A., McIntosh, J.M., Ghelardini, C., 2014. α-Conotoxin RgIA protects against the development of nerve injury-induced chronic pain and prevents both neuronal and glial derangement. Pain 155, 1986–1995. https://doi.org/10.1016/j.pain.2014.06.023.

Di Cesare Mannelli, L., Lucarini, E., Micheli, L., Mosca, I., Ambrosino, P., Soldovieri, M.V., Martelli, A., Testai, L., Taglialatela, M., Calderone, V., Ghelardini, C., 2017. Effects of natural and synthetic isothiocyanate-based H_2S-releasers against chemotherapy-induced neuropathic pain: role of Kv7 potassium channels. Neuropharmacology 121, 49–59. https://doi.org/10.1016/j.neuropharm.2017.04.029.

Elgoyhen, A.B., Katz, E., Fuchs, P.A., 2009. The nicotinic receptor of choclear hair cells: a possible pharmacotherapeutic target? Biochem. Pharmacol. 78 (7), 712–719. https://doi.org/10.1016/j.bcp.2009.05.023.

Fujii, T., Mashimo, M., Moriwaki, Y., Misawa, H., Ono, S., Horiguchi, K., Kawashima, K., 2017. Expression and function of the cholinergic system in immune cells. Front. Immunol. 8, 1085. https://doi.org/10.3389/fimmu.2017.01085.

Grishin, A.A., Wang, C.I.A., Muttenthaler, M., Alewood, P.F., Lewis, R.J., Adams, D.J., 2010. α-Conotoxin AuIB isomers exhibit distinct inhibitory mechanisms and differential sensitivity to stoichiometry of α3β4 nicotinic acetylcholine receptors. J. Biol. Chem. 285, 22254–22263. https://doi.org/10.1074/jbc.M110.111880.

Guerrini, G., Ciciani, G., Crocetti, L., Daniele, S., Ghelardini, C., Giovannoni, M.P., Iacovone, A., Di Cesare Mannelli, L., Martini, C., Vergelli, C., 2017. Identification of a new pyrazolo[1,5-a]quinazoline ligand highly affine to γ-aminobutyric type A ($GABA_A$) receptor subtype with anxiolytic-like and antihyperalgesic activity. J. Med. Chem. 60, 9691–9702. https://doi.org/10.1021/acs.jmedchem.7b01151.

Halai, R., Clark, R.C., Nevin, S.T., Jensen, J.E., Adams, D.J., Craik, D.J., 2009. Scanning mutagenesis of α-conotoxin Vc1.1 reveals residues crucial for activity at the α9α10 nicotinic acetylcholine receptor. J. Biol. Chem. 284, 20275–20284. https://doi.org/10.1074/jbc.M109.015339.

Hone, A.J., McIntosh, J.M., 2018. Nicotinic acetylcholine receptors in neuropathic and inflammatory pain. FEBS Lett. 592, 1045–1062. https://doi.org/10.1002/1873-3468.12884.

Jadhav, A., Liang, W., Papageorgiou, P.C., Shoker, A., Kanthan, S.C., Balsevich, J., Levy, A.S., Heximer, S., Backx, P.H., Gopalakrishnan, V., 2013. Catharanthine dilates small mesenteric arteries and decreases heart rate and cardiac contractility by inhibition of voltage-operated calcium channels on vascular smooth muscle cells and cardiomyocytes. J. Pharmacol. Exp. Therapeut. 345, 383–392. https://doi.org/10.1124/jpet.112.199661.

Koenig, X., Kovar, M., Rubi, L., Mike, A.K., Lukacs, P., Gawali, V.S., Todt, H., Hilber, K., Sandtner, W., 2013. Anti-addiction drug ibogaine inhibits voltage-gated ionic currents: a study to assess the drug's cardiac ion channel profile. Toxicol. Appl. Pharmacol. 273, 259–268. https://doi.org/10.1016/j.taap.2013.05.012.

Kumburovic, K., Selakovic, D., Juric, T., Jovicic, N., Mihailovic, M., Stankovic, J.K., Sreckovic, N., Kumburovic, D., Jakovljevic, V., Rosic, G., 2019. Antioxidant effects of *Satureja hortensis* L. attenuate the anxiogenic effect of cisplatin in rats. Oxidative Medicine and Cellular Longevity. https://doi.org/10.1155/2019/8307196. 2019.

Lee, S., 2013. Pharmacological inhibition of voltage-gated Ca^{2+} channels for chronic pain relief. Curr. Neuropharmacol. 11, 606–620. https://doi.org/10.2174/1570159X11311060005.

Lees, J.G., Makker, P.G., Tonkin, R.S., Abdulla, M., Park, S.B., Goldstein, D., Moalem-Taylor, G., 2017. Immune-mediated processes implicated in chemotherapy-induced peripheral neuropathy. Eur. J. Canc. 73, 22–29. https://doi.org/10.1016/j.ejca.2016.

12.006.
Liang, J., Tae, H.S., Xu, X., Jiang, T., Adams, D.J., Yu, R., 2020. Dimerization of α-conotoxins as a strategy to enhance the inhibition of the human α7 and α9α10 nicotinic acetylcholine receptors. J. Med. Chem. 63, 2974–2985. https://doi.org/10.1021/acs.jmedchem.9b01536.
Lin, C., Cai, J., Yang, X., Hu, L., Lin, G., 2015. Liquid chromatography mass spectrometry simultaneous determination of vindoline and catharanthine in rat plasma and its application to a pharmacokinetic study. Biomed. Chromatogr. 29, 97–102. https://doi.org/10.1002/bmc.3244.
Maisonneuve, I.M., Glick, S.D., 2003. Anti-addictive actions of an iboga alkaloid congener: a novel mechanism for a novel treatment. Pharmacol. Biochem. Behav. 75, 607–618. https://doi.org/10.1016/s0091-3057(03)00119-9.
McIntosh, J.M., Absalom, N., Chebib, M., Elgoyhen, A.B., Vincler, M., 2009. α9 nicotinic acetylcholine receptors and the treatment of pain. Biochem. Pharmacol. 78, 693–702. https://doi.org/10.1016/j.bcp.2009.05.020.
Romero, H.K., Christensen, S.B., Di Cesare Mannelli, L., Gajewiak, J., Ramachandra, R., Elmslie, K.S., Vetter, D.E., Ghelardini, C., Iadonato, S.P., Mercado, J.L., Olivera, B.M., McIntosh, J.M., 2017. Inhibition of α9α10 nicotinic acetylcholine receptors prevents chemotherapy-induced neuropathic pain. Proc. Natl. Acad. Sci. U. S. A. 114, E1825–E1832. https://doi.org/10.1073/pnas.1621433114.
Sadeghi, M., Carstens, B.B., Callaghan, B.P., Daniel, J.T., Tae, H.S., O'Donnell, T., Castro, J., Brierley, S.M., Adams, D.J., Craik, D.J., Clark, R.J., 2018. Structure-activity studies reveal the molecular basis for $GABA_B$-receptor mediated inhibition of high voltage-activated calcium channels by α-conotoxin Vc1.1. ACS Chem. Biol. 13, 1577–1587. https://doi.org/10.1021/acschembio.8b00190.
Ta, L.E., Low, P.A., Windebank, A.J., 2009. Mice with cisplatin and oxaliplatin-induced painful neuropathy develop distinct early responses to thermal stimuli. Mol. Pain 5, 9. https://doi.org/10.1186/1744-8069-5-9.
Taraschenko, O.D., Rubbinaccio, H.Y., Maisonneuve, I.M., Glick, S.D., 2008. 18-methoxycoronaridine: a potential new treatment for obesity in rats? Psychopharmacology (Berlin) 201, 339–350. https://doi.org/10.1007/s00213-008-1290-9.
Vaught, J.L., Pelley, K., Costa, L.G., Setler, P., Enna, S.J., 1985. A comparison of the antinociceptive responses to the GABA-receptor agonists THIP and baclofen. Neuropharmacology 24, 211–216. https://doi.org/10.1016/0028-3908(85)90076-0.
Winquist, R.J., Pan, J.Q., Gribkoff, V.K., 2005. Use-dependent blockade of CaV2.2 voltage-gated calcium channels for neuropathic pain. Biochem. Pharmacol. 70, 489–499. https://doi.org/10.1016/j.bcp.2005.04.035.
Yu, R., Tae, H.S., Tabassum, N., Shi, J., Jiang, T., Adams, D.J., 2018. Molecular determinants conferring the stoichiometric-dependent activity of α-conotoxins at the human α9α10 nicotinic acetylcholine receptor subtype. J. Med. Chem. 61, 4628–4634. https://doi.org/10.1021/acs.jmedchem.8b00115.
Zamponi, G.W., Striessnig, J., Koschak, A., Dolphin, A.C., 2015. The physiology, pathology, and pharmacology of voltage-gated calcium channels and their future therapeutic potential. Pharmacol. Rev. 67, 821–870. https://doi.org/10.1124/pr.114.009654.
Zoli, M., Pucci, S., Vilella, A., Gotti, C., 2018. Neuronal and extraneuronal nicotoinic acetylcholine receptors. Curr. Neuropharmacol. 16 (4), 338–349. https://doi.org/10.2174/1570159X15666170912110450.